Bacterial RNase P: a new view of an ancient enzyme

Alexei V. Kazantsev and Norman R. Pace

Abstract | Ribonuclease P (RNase P) is a ubiquitous endonuclease that catalyses the maturation of the 5′ end of transfer RNA (tRNA). Although it carries out a biochemically simple reaction, RNase P is a complex ribonucleoprotein particle composed of a single large RNA and at least one protein component. In bacteria and some archaea, the RNA component of RNase P can catalyse tRNA maturation *in vitro* in the absence of proteins. The discovery of the catalytic activity of the bacterial RNase P RNA triggered numerous mechanistic and biochemical studies of the reactions catalysed by the RNA alone and by the holoenzyme and, in recent years, structures of individual components of the RNase P holoenzyme have been determined. The goal of the present review is to summarize what is known about the bacterial RNase P, and to bring together the recent structural results with extensive earlier biochemical and phylogenetic findings.

Ribozyme
An enzyme that has an RNA as the catalytic component. RNase P belongs to the large ribozyme class, which also includes the self-splicing group-I and group-II introns.

4.5S RNA
In bacteria, the signal-recognition particle comprises 4.5S RNA and the Ffh protein.

Transfer messenger RNA
(Tm RNA). Also known as SsrA. Involved in a *trans*-translation process that adds a C-terminal peptide tag to unfinished proteins at stalled ribosomes that targets the unfinished proteins for proteolysis.

Department of Molecular, Cellular and Developmental Biology, University of Colorado, Boulder, Colorado 80309-0347, USA. Correspondence to N.R.P. e-mail: Norman.Pace@colorado.edu
doi:10.1038/nrmicro1491

Ribonuclease P (RNase P) catalyses the maturation of the 5′ end of transfer RNA (tRNA) (BOX 1). It is a ubiquitous endonuclease that is found in cells from all three domains of life: the Bacteria, Eukarya and Archaea[1,2]. RNase P carries out a simple enzymatic reaction: the hydrolysis of a specific phosphodiester bond in precursor tRNAs (pre-tRNAs) to release the 5′-precursor sequence and thereby generate tRNAs with mature 5′ ends (FIG. 1a).

This simple reaction requires a remarkably complex and unusual enzyme. What is unusual about RNase P is that it is one of only a few ribonucleoprotein enzymes. In bacteria and some archaea, the RNA component of RNase P can catalyse tRNA maturation *in vitro* in the absence of proteins[3,4]. RNase P is, therefore, an RNA-based enzyme, or ribozyme.

RNase P is required for cell viability: both the RNA and protein components of RNase P are essential *in vivo*[5–8]. The protein composition of the RNase P holoenzyme differs markedly between the bacterial (1 small basic protein), archaeal (4 or 5 different protein subunits) and eukaryal (10 different protein components) versions of the enzyme[9]. Most structural and mechanistic studies have focused on the bacterial version because of its relative simplicity and the fact that the RNA component is catalytic. The eukaryal RNase P is reviewed elsewhere[2,10,11] and RNase P has been reviewed extensively over the years[9,12–14]. The goal of this review is to summarize what is known about bacterial RNase P, and to bring together recent structural results and extensive earlier biochemical and phylogenetic findings. Collectively, the results reveal a new perspective on this remarkable enzyme.

In contrast to other large natural ribozymes, such as group-I and group-II introns, RNase P conducts multiple turnovers *in vivo*. The other ribozymes carry out 'one-shot' reactions that involve rearrangements of RNA structure and the making and breaking of phosphodiester bonds. RNase P and the ribosome are the only known ribozymes that naturally conduct multiple catalytic cycles. Another distinctive feature of RNase P is its ability to process various different substrates correctly (BOX 2), including all the different pre-tRNAs (which in some cells amount to more than 100) and, in bacteria, the 4.5S RNA[15], bacteriophage ϕ80-induced RNA[16], the 3′-terminal structure of the turnip yellow mosaic virus genomic RNA[17], transfer messenger RNA (tmRNA)[18], the mRNA from the polycistronic *his* operon[19], the pre-C4 repressor RNA from bacteriophages P1 and P7 (REF. 20), and some transient structures adopted by riboswitches[21]. These alternative substrates for RNase P have not been well characterized, but all probably mimic the primary substrate, pre-tRNA, in some way. Perhaps this versatility in substrate selection explains the complex nature of RNase P.

The discovery of the catalytic activity of the RNA of bacterial RNase P in 1983 (REF. 3) triggered numerous mechanistic and biochemical studies of reactions catalysed by RNA alone and those catalysed by the

Riboswitch
A regulatory structure in an mRNA molecule that undergoes a conformational change induced by the binding of a small metabolite, and which results in activation or inactivation of the mRNA.

S_N2 nucleophilic reaction
A bimolecular nucleophilic substitution reaction that involves displacement of a leaving group by an attacking nucleophile. An S_N2 reaction that involves phosphate esters (for example, an internucleotide phosphodiester) proceeds through the formation of a trigonal bipyramidal transition state.

Quench-flow technique
A technique that allows the analysis of chemical reactions at the millisecond time scale.

Hill analysis
A common technique that analyses cooperative binding of ligands to biomacromolecules (proteins and nucleic acids). Either equilibrium binding (for example, extent of saturation) or the rate of the ligand-dependent enzymatic reaction is followed as a function of the concentration of the ligand. Mathematical analysis of the binding function yields the number of cooperatively bound ligands as well as the affinity constant.

Phosphorothioate substitution
A common chemical modification that substitutes a sulphur atom for one of the non-bridging oxygens in the phosphodiester linkage.

Thiophilic
Having a high affinity for sulphur.

Kinetic isotope-effect study
A kinetic isotope effect is a change in the rate of a chemical reaction owing to a substitution of a participating chemical group with an analogue that contains a different isotope of one of the constituent atoms. As kinetic isotope effects reflect changes in the vibration energy of the transition state of the reaction caused by substitution, they are a useful tool for studying the mechanism of chemical reactions.

Box 1 | **Maturation and architecture of tRNA**

All transfer RNAs (tRNAs) are synthesized as inactive precursors that have to undergo extensive post-transcriptional maturation prior to their incorporation into cellular metabolism. Maturation of tRNA includes: the removal of extraneous 5′ and 3′ nucleotides by a set of endonucleases and exonucleases; addition of the 3′-CCA by terminal transferase; removal of the intervening sequences; and an extensive number of nucleotide modifications (up to 20% of nucleotides in typical tRNA are modified). Approximately 100 different nucleotide modifications are known; the most common include the formation of pseudouridine and methylation of the bases and the ribose. Our understanding of the biochemical functions of the tRNA modifications is far from complete. Some modifications have been shown to enforce correct folding of the tRNA by suppressing the formation of alternative structures; modifications of the nucleotides at the anticodon are known to improve the fidelity of translation. However, many modifications in tRNA seem 'cryptic', as knockout of the genes responsible for these modifications results in no detectable phenotype.

The global organization of the tRNA structure is highly conserved in all forms of life. Prominent features of the tRNA structure, as shown in the figure, include: an acceptor stem with the CCA trinucleotide at the 3′ end (the site of aminoacylation and *trans*-peptidation reactions in the protein-biosynthesis cycle); a D loop (named after a tandem dihydrouridine modification, labelled 'D' in the figure, which is commonly found in this loop); an anticodon loop that includes the anticodon, which is a nucleotide triplet responsible for recognition of a coding triplet in mRNA, and the TΨC loop (or T loop), named after the highly conserved triplet TΨC. Filled circles represent nucleotides that are not usually modified; open circles represent commonly modified nucleotides other than D, T and Ψ.

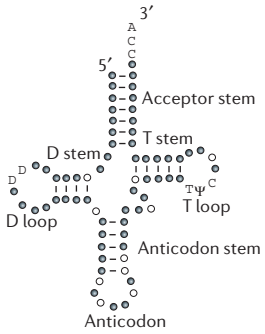

holoenzyme. The interpretation of many of the results of these studies has been hampered by the lack of a detailed structural perspective beyond that provided by comparative sequence analysis. It was not even clear which nucleotides in the RNA would constitute the chemically active site. In recent years, structures of the individual components of the RNase P holoenzyme have been determined by nuclear magnetic resonance (NMR) and X-ray crystallography, and an entirely new structural perspective on the function of RNase P has begun to emerge.

The chemistry of RNase P catalysis

RNase P catalyses the hydrolysis of a phosphodiester bond, to generate a phosphate at the 5′ end of mature tRNA[22] and a precursor sequence with a terminal 2′–3′-*cis*-glycol (FIG. 1). Our current understanding of the structure of the transition state of the RNase P-catalysed reaction is summarized in FIG. 1b. In this model, the labile phosphodiester bond is encaged by Mg^{2+}-hydrate coordinate complexes to form a trigonal bipyramidal transition state, and the 2′-OH of the precursor tRNA domain facilitates protonation of the leaving 3′-oxygen. The available biochemical data are consistent with this concerted S_N2-like nucleophilic substitution mechanism[23–26] (BOX 3). There is no evidence for formation of a covalent intermediate involving the substrate and ribozyme RNAs.

The rate of the chemical step of catalysis, measured under single-turnover conditions, increases with pH and is approximately first-order in the pH range 6–8. This is consistent with either an enzyme-bound hydroxide-ion nucleophile or a general base-catalysed hydrolysis mechanism. At a pH of 6, the rate of the chemical step is sufficiently slow (~2 min^{-1}) for pre-steady-state kinetic analysis to be conducted by conventional 'manual' techniques; the results of such analyses can be extrapolated to more physiologically relevant pH values and generally agree with the analyses performed by rapid quench-flow techniques at a pH of 8 (rate of chemical step ~5 s^{-1}). This overall turnover rate of RNase P is slow compared with the turnover rate of enzymes that have evolved to function at high catalytic efficiency. Consequently, it has been suggested that RNase P has been optimized for cleavage-site selectivity and for recognition of several different substrates rather than for rapid catalysis[24].

Catalysis by RNase P RNA is absolutely dependent on divalent metal ions, notably Mg^{2+} or Mn^{2+} (REF. 27), although others, such as Ca^{2+}, Zn^{2+} and Pb^{2+}, usually in combinations with Ba^{2+}, Sr^{2+} or $Co(NH_3)_6^{3+}$, have been reported to sustain some catalytic activity[27–30]. Hill analyses of the dependence of the chemical rate on the concentration of Mg^{2+} ions indicates stabilization of the transition state by up to three cooperatively bound Mg^{2+} ions, consistent with the mechanistic model shown in FIG. 1b[23,31]. Because divalent metal ions are also required for the folding of the enzyme[32–34] and for substrate binding[31], interpreting the metal-ion dependence in terms of catalysis is not straightforward. The metalloenzyme nature of RNase P is supported, however, by studies of the cleavage of pre-tRNAs that contain R_p-phosphorothioate substitutions at the substrate phosphodiester bond. This switches the metal-ion specificity of the chemically active site to preferentially use thiophilic metal ions (Cd^{2+} or Mn^{2+})[35,36]. Substitution of the pro-R_p non-bridging phosphate oxygen with sulphur results in a significant (~10^4 fold) reduction in the catalytic activity of the Mg^{2+}-supported reaction. However, the catalytic activity is mostly restored by substitution of the Mg^{2+} ion with the more thiophilic Cd^{2+} or Mn^{2+}, and Hill analysis of the Cd^{2+}-dependence of this 'rescue' reaction indicates direct cooperative coordination of two Cd^{2+} ions to the R_p-sulphur in the transition state. The results of kinetic isotope-effect studies are also consistent with the metalloenzyme nature of RNase P RNA and indicate direct coordination of the hydroxide-ion nucleophile to the enzyme-bound Mg^{2+} ion at the transition state of the reaction[26].

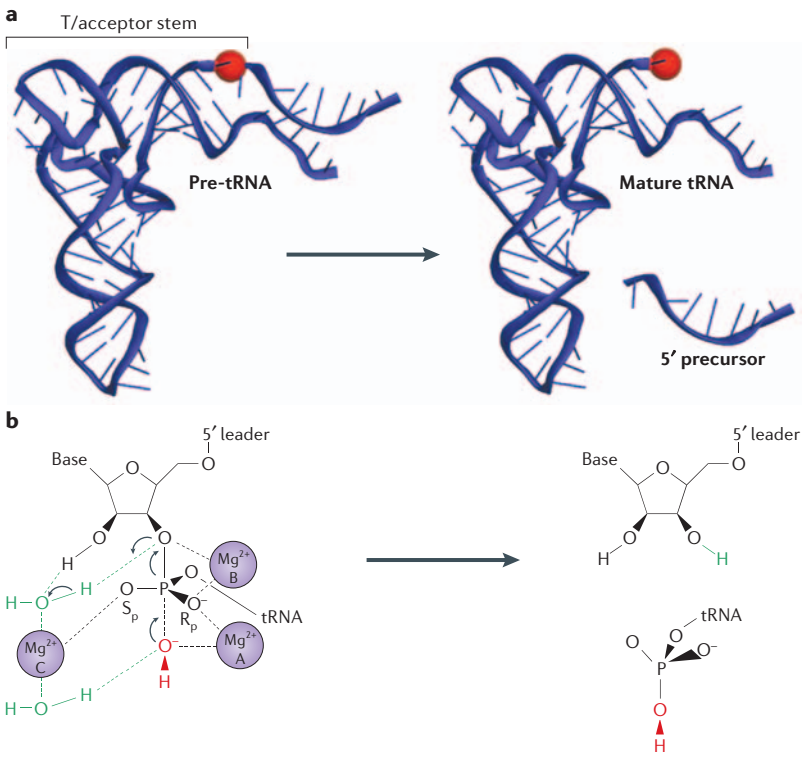

Figure 1 | **RNase P catalyses maturation of the 5′end of tRNA. a** | RNase P catalyses the hydrolysis of a phosphodiester bond in precursor transfer RNA (pre-tRNA) to release the 5′-precursor sequence and generate tRNAs with mature 5′ ends. A cartoon representation of pre-tRNA is shown on the left and the products of the reaction, mature tRNA and the 5′ precursor, are shown on the right. The substrate phosphate is indicated by a red sphere. **b** | The proposed mechanism of the reaction based on biochemical studies. On the left is a putative structure of the transition state of the reaction. The electron flow is indicated by arrows. The pro-R_p oxygen of the scissile phosphate coordinates two Mg^{2+} ions, A and B. Ion A activates and positions the nucleophile (the hydroxide ion, shown in red) and ion B stabilizes the transition state and activates the 3′-oxygen leaving group by neutralizing a developing negative charge. The third Mg^{2+} ion, C, has been proposed to coordinate to the 2′-OH of the preceding nucleotide (N_{-1}), through inner-sphere water (shown in green), and to contribute to activation of the leaving group by lowering the pK_a of the coordinated water molecule and thereby alleviating the proton transfer to the 3′ oxygen. pK_a, dissociation constant of an acid.

A wealth of accumulated biochemical data are consistent with the notion that RNase P uses some version of the two-metal-ion mechanism of catalysis[37] that is characteristic of many other phosphoryl-transfer enzymes, both RNA and protein[38]. Other enzymes that use the two-metal-ion mechanism include group-I self-splicing introns[39], DNA and RNA polymerases[40,41], RNase H[42], and restriction and homing endonucleases[43,44]. However, the RNase P-catalysed reaction seems to be a variation on this mechanism. Apparently, the substrate 2′-OH at the site of cleavage is involved in coordination of a third catalytic metal ion, as shown in FIG. 1b. This is evidenced by the finding that removal of the 2′-OH by substitution with the 2′-deoxynucleotide next to the cleaved bond substantially reduces the rate of cleavage and lowers cooperativity for the catalytic metal ions[23].

Therefore, although we have considerable information about the chemistry of the RNase P reaction, the nature and the arrangement of the chemical groups provided by the enzyme are missing from the picture. A major challenge for our understanding of the enzymology of RNase P is unravelling the detailed structural basis for substrate recognition and catalysis. Studies over the past two decades, initially by phylogenetic comparative analysis and most recently by crystallography, have provided an increasingly detailed view of the structures of the RNase P components.

Phylogenetic variation and RNase P RNA structure

Phylogenetic comparative analysis[45] provided most of the overall secondary-structure data well before crystallographic analysis of RNase P was possible. A fundamental building block of RNA structure is the anti-parallel, double-stranded helix. Evolutionary conservation of any helical structure is achieved by maintaining base-paired interactions between nucleotides to form a helix, which functions as a structural barrel. Consequently, in an alignment of diverse but homologous RNA sequences (that is, sequences of common ancestry), base-paired interactions can be identified as pairs of nucleotides that co-vary usually to preserve Watson–Crick complementarity. Stretches of such co-varying pairs are expected to form the double-stranded helices of secondary structure[46]. As an analysis of RNA secondary structure is refined by multiple iterations of such co-variation analysis with many diverse sequences, further structural information can be extracted by identifying known RNA motifs and long-range interactions that involve isolated base pairs and base triplets[47].

The current perspective on the secondary structure of the bacterial RNase P RNA has been refined incrementally by comparative analysis of more than 100 sequences from phylogenetically diverse bacteria[48,49]. The gross structural variation among different bacterial groups is shown in FIG. 2. There are two main structural types of bacterial RNase P RNA: the A type (ancestral type) and the B type (*Bacillus* type) (FIGS 2,3). Despite some significant differences in the structure of their peripheral elements, all bacterial RNase P RNAs share a set of highly conserved structural elements that are represented by the phylogenetic minimal structure shown in FIG. 2b. A synthetic minimal RNase P structure, which can be engineered by removal of the non-core elements from the RNA of a native RNase P using molecular cloning techniques, is catalytically active[50]. Therefore, these conserved structural elements are expected to constitute the structural and functional core of the ribozyme.

Many nucleotides in the structural core of RNase P are highly conserved, implying that they are functionally important. Most of the highly conserved nucleotides occur in five regions of sequence conservation, conserved regions (CRs) I-V (FIG. 2b). These CRs tend to occur in sequences that connect helical elements, although parts of CRI and CRV base-pair and are involved in formation of the highly conserved helical element P4 (FIG. 2b).

Phylogenetically variable structural elements, in turn, have been implicated in the formation of long-range docking interactions that are expected to stabilize the overall conformation of the ribozyme. For example, the minimal phylogenetic structure produced by whittling down these variable elements from a native RNA resulted

RNase H
An endoribonuclease that specifically hydrolyses the phosphodiester bonds of RNA that are hybridized to DNA. Does not digest single-stranded or double-stranded DNA.

Homing endonucleases
A large class of endonuclease that recognize a specific sequence that flanks the homing endonuclease-encoding gene, but only when the homing endonuclease-encoding gene itself does not interrupt this sequence.

Box 2 | **Alternative substrates for RNase P**

The world of small RNAs is rapidly expanding and some have been found to be processed by ribonuclease P (RNase P). The most well studied of these alternative substrates for RNase P are the transfer messenger RNA (tmRNA) and the 4.5S RNA. As with tRNA, both of these small RNAs are involved at different stages of protein biosynthesis.

tmRNA. The tmRNA or SsrA RNA (also known as 10Sa RNA) is a 350–400 nucleotide RNA involved in the process that rescues ribosomes that are stalled at aberrantly terminated mRNA and targets the incompletely synthesized protein for degradation. As its name suggests, the tmRNA has elements of tRNA and mRNA in its structure. The 5′ and 3′ ends of the molecule form a tRNA-like domain (or TLD) that structurally and functionally resembles tRNA; it is the 5′ end of the TLD that is generated by RNase P. Similar to tRNA, the CCA at the 3′ end of the TLD of the tmRNA is aminoacylated with alanine. The mRNA-like part includes mostly a single-stranded stretch of RNA that encodes a signal oligopeptide and a stop codon. When a translating ribosome encounters an aberrant termination of the mRNA chain (in which the template ends before a stop codon is encountered), it stalls. A ribonucleoprotein particle composed of tmRNA and a small protein SmpB is then loaded onto the stalled ribosome and the alanine at the 3′ end of the tmRNA is added to the translated polypeptide. Translation then resumes on the tmRNA template until the ribosome encounters the stop codon. The defective message is degraded and the defective protein, now tagged with a degradation signal, is digested by cellular proteases.

4.5S RNA. The 4.5S RNA in bacteria is a small (~150 nucleotides) highly structured RNA that is part of the signal-recognition particle (SRP), a universally conserved ribonucleoprotein that mediates co-translational transmembrane translocation of proteins. Newly synthesized secreted and transmembrane proteins contain a hydrophobic signal sequence, usually at the N terminus. SRP binds the signal peptide that emerges from the exit tunnel on the ribosome and induces translation arrest. The SRP complexed with the ribosome is bound by the membrane-associated SRP receptor that loads the ribosome onto a translocational complex on the membrane. On binding to the translocational complex, the ribosome resumes translation and the newly synthesized protein is secreted as it is exits from the ribosome. The SRP is released from the receptor and the cycle continues.

in a catalytically active RNase P RNA, but one that was severely destabilized in its tertiary structural packing[50].

Co-variation analysis has proven that about two-thirds of any bacterial RNase P RNA is involved in the formation of anti-parallel, double-stranded helices of a predictable structure (an A-form helix). An insight into the overall structural organization of this ribozyme was achieved by modelling these helical barrels in three dimensions based on long-range distance constraints that were obtained from phylogenetic information on long-range co-variations and biochemical photo-affinity crosslinking data[51–54]. The resulting models, which were developed independently by different groups almost a decade ago, predicted that, despite significant structural differences, A-type and B-type RNase P RNAs fold into globally similar three-dimensional structures[55,56].

Box 3 | **Ribozyme-catalysed reactions**

With the exception of the ribosome, all natural ribozymes catalyse *trans*-esterification reactions at the phosphorous atom (also known as phosphoryl-transfer reactions). These ribozyme-catalysed reactions result in hydrolysis, ligation or substitution at a specific internucleotide phosphate in nucleic acids, most commonly in RNA. Although all these reactions proceed through an S_N2-like mechanism, they can be subdivided into two main classes according to the chemical nature of the participating phosphate species.

The first class includes reactions that involve 2′–3′-cyclic phosphates that are either formed as a result of the cleavage of internucleotide phosphate or are the substrates for a reverse-ligation reaction. The nucleophile that attacks the reactive phosphate group is either the 2′-OH at the site of chain cleavage or the 5′-OH in the case of the reverse-ligation reaction, and it is the covalent bond between the reacting phosphorous atom and the 5′-oxygen atoms that is broken or formed. These reactions are thought to be mechanistically similar to a well-studied RNA-cleavage reaction catalysed by the protein-based ribonuclease A (RNase A). The ribozymes that catalyse these reactions are known as small ribozymes (their typical sizes range from ~70 to ~200 nucleotides) and include hammerhead ribozymes, hairpin ribozymes, hepatitis delta ribozymes, the Glm-riboswitch ribozyme and the *Neurospora* VS ribozyme. Although divalent metal ions stimulate catalysis by small ribozymes, they are not absolutely required for the chemical step and are thought to participate in energetic stabilization of the catalytically competent ribozyme structure.

The second class of reaction that is catalysed by natural ribozymes does not involve the 2′–3′-cyclic phosphates. The 2′-OH, 3′-OH or activated water molecule functions as a nucleophile and the covalent bond between the reacting phosphorous atom and the 5′-oxygen atoms remains intact. These reactions are thought to be mechanistically similar to nucleic-acid polymerization as catalysed by DNA and RNA polymerases, as well as to the hydrolytic reactions catalysed by RNase H and restriction and homing endonucleases. The ribozymes that catalyse these reactions are known as large ribozymes (typical sizes range from ~300 to more than 800 nucleotides) and include group-I and group-II self-splicing introns and RNase P. These large RNAs can show catalytic properties *in vitro*, but they are generally stimulated by or require one or more protein cofactors *in vivo*. All phosphoryl-transfer reactions of this class have a mechanistic requirement for divalent metal ions that are thought to participate directly in the chemical step by contributing to the activation of the nucleophile, stabilization of the leaving group and by electrostatic stabilization of the transition state.

Although the chemical mechanisms that are used by ribozymes seem to correlate with the sizes of these catalytic RNAs, there is no obvious reason why this should be so.

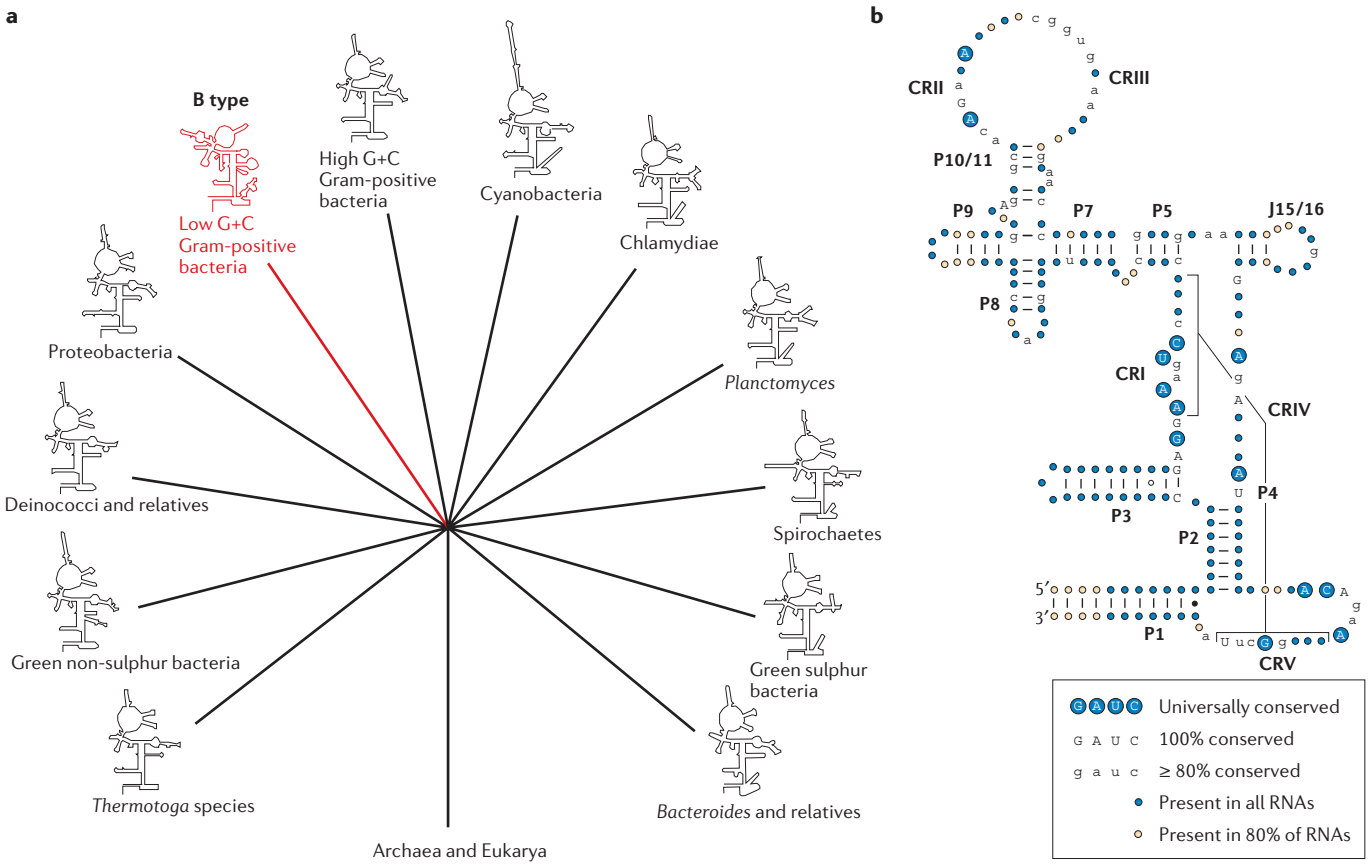

Figure 2 | **Phylogenetic variation and nucleotide conservation among bacterial RNase P RNAs. a** | Distribution of the secondary structures of ribonuclease P (RNase P) RNA among major bacterial groups. **b** | The phylogenetic minimal structure outlines a structurally conserved core of the bacterial RNase P RNA. Paired regions representing double-stranded helices are labelled P1, P2, and so on, in the order of their appearance from the 5′-end of the sequence. The interhelical joining regions, for example, J15/16, are labelled according to the names of the paired regions that they connect. CRI–V, conserved regions I–V.

The development of a well-refined secondary structure for the bacterial RNase P RNA also provided a framework for analysis of the archaeal and eukaryal counterparts. RNase P RNAs from all three domains of life clearly have a common origin and share most of the highly conserved elements that were originally identified in the bacterial RNase P RNA[57–59]. In contrast to the bacterial RNase P RNA, however, RNase P RNAs from eukaryotes and most archaea are catalytically inactive without the protein components[4]. Nonetheless, the universal conservation of the core structural elements indicates that, despite the fact that some forms of the RNA lack *in vitro* ribozyme activity, the catalytic function of all ribonucleoprotein-based RNase P species is intrinsically associated with the RNA component. Consistent with this, the RNA-containing eukaryal RNase P holoenzymes are mechanistically similar to the bacterial ribozyme: the same R_p-phosphorothioate modification in the substrate at the cleavage site markedly reduces the rate of hydrolysis and this interference is rescued by the presence of thiophilic Cd^{2+} or Mn^{2+} ions[60,61]. This indicates that the active site of bacterial and eukaryal RNase P share a common organization. By contrast, the only known protein-based RNase-P-like activity, that of the spinach chloroplast, is not inhibited by the R_p-phosphorothioate modification of the substrate phosphodiester[62]. This implies a distinctly different mechanism of catalysis than that used by the ribozyme.

Crystal structures of RNase P RNA

In recent years our understanding of the bacterial RNase P structure has been significantly advanced by several structures solved by X-ray crystallography. Low-resolution X-ray crystal structures of full-size RNase P RNAs from *Thermotoga maritima* (A type)[63] and *Bacillus stearothermophilus* (B type)[64] have been solved, as well as the structures of an independently folding S domain[32,65] from the *Thermus thermophilus* (A type)[66] and *Bacillus subtilis* (B type)[67] RNase P RNAs. None of these RNA structures is sufficiently flawless to give us a unique perspective on the structure of the catalytically active RNase P RNA conformation. Comparison of the structural elements that are common between the different structures reveals some technical problems with each of the structures. Therefore, a comparative approach to thinking about RNase P RNA structure is required.

The *B. stearothermophilus* structure could be resolved to 3.3 Å and so revealed much structural detail that could not be seen in the *T. maritima* structure at 3.85 Å. A comparison of these two models is shown in FIG. 3. A major disadvantage of the *B. stearothermophilus* structure is the disorder of a large part of its S domain and, therefore, the lack of crystallographic data with which to infer the structure of this part of the molecule. The full-size B-type RNase P RNA structure can, however, be reconstructed by superimposing an overlapping, independently solved structure of the S domain from *B. subtilis*. This results in differences in the positioning of some of the S domain in the full-length A-type and B-type RNAs (FIG. 3). A folding problem that is apparent in the structure of the RNA from *T. maritima* RNase P is that the A-type-specific helical element P6 docks *in trans* between two symmetrically related molecules in the crystal. Formation of the dimer in the crystal structure disrupts a large structural element — a long-range stabilizing interaction that consists of P15, P16, P17 and P6 — which results in a misfolded conformation. As RNase P RNA is active as a monomer *in vitro*[68,69], such dimerization is presumably biologically irrelevant. In turn, each of the independently solved S-domain structures is distorted by the absence of anchor points in the C domain of the RNase P RNA. Taken together, however, the collection of crystal structures provides a novel view of the RNase P RNA.

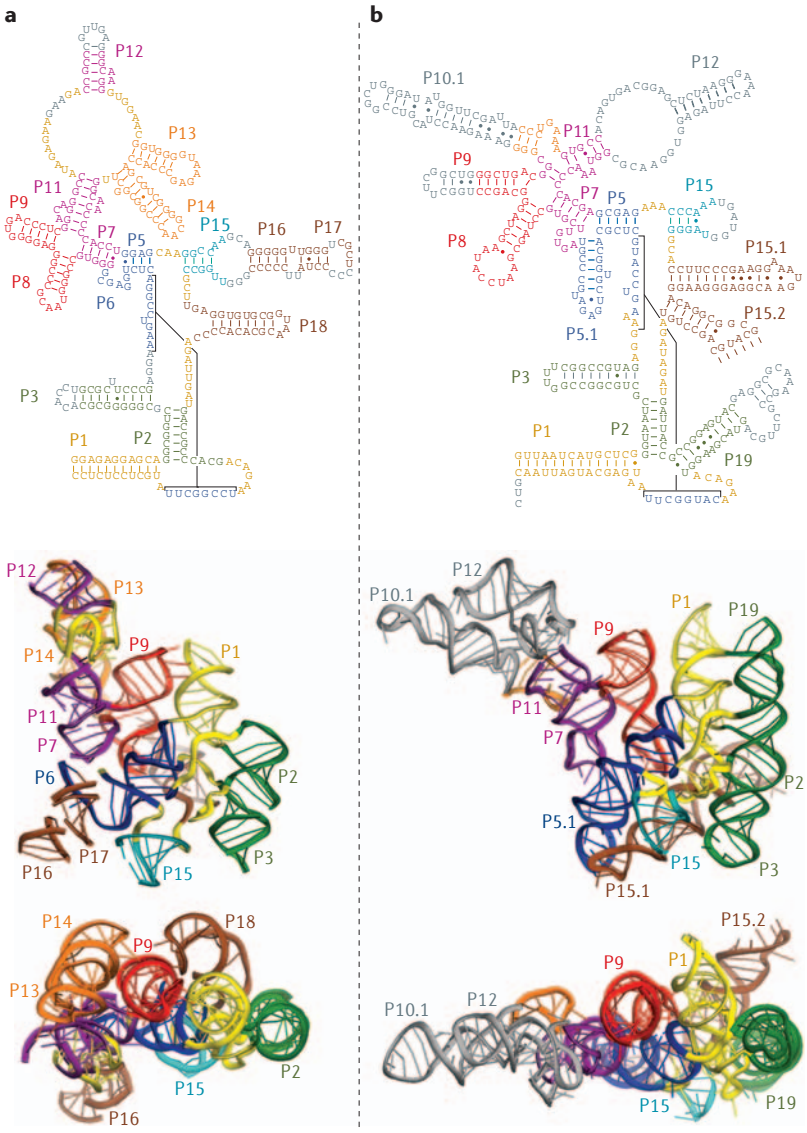

Figure 3 | **Comparison of the crystal structures of the A-type and B-type RNase P RNAs. a** | The secondary structure and a ribbon diagram of a model of the A-type RNA of the *Thermotoga maritima* ribonuclease P (RNase P) (PDB ID 2A2E). Elements of the secondary structure (top panel) are coloured according to their involvement in the formation of the coaxially stacked helical domains of the crystal structure. Nucleotides coloured in grey in the secondary structure are disordered in the crystal and could not be modelled. **b** | The secondary structure and a ribbon diagram of a model of the B-type RNA of the *Bacillus stearothermophilus* RNase P (PDB ID 2A64). The coaxially stacked helical domains are coloured according to their homology to the A-type RNA. Nucleotides coloured in grey in the secondary structure are disordered in the crystal and could not be modelled. A large structural element coloured in grey in the ribbon diagram is disordered in the crystal and was modelled by superimposition with a homologous crystal structure of the S domain from *Bacillus subtilis* (PDB ID 1NBS). The panels on the bottom show that the coaxially stacked helical domains, coloured in green, yellow, blue, red and purple, form a remarkably flat substrate-binding surface in both A-type and B-type RNAs.

What do the structures shown in FIG. 3 tell us about the biologically relevant structural organization of RNase P RNA? Both A-type and B-type RNase P RNAs are formed by coaxially stacked helical domains, which are joined together by long-range docking interactions. The spatial arrangement of these coaxially stacked helices is highly similar between A-type and B-type RNAs (FIG. 3) and, in both cases, results in a compactly folded RNA with a remarkably flat surface to which the substrate pre-tRNA binds. Phylogenetically variable structural elements are located on the surface of the core structure, away from the substrate-binding face, and tend to participate in long-range docking interactions that, as mentioned above, provide global structural stability. Differences in the docking elements might explain some gross differences in the structures of A-type and B-type RNAs. The S domain, for example, is well ordered in the A-type RNA structure (FIG. 3a), apparently as the result of long-range docking of the A-type specific element P14 to the universally present helix P8. An equivalent long-range structure does not occur in the B-type RNA, which might explain why the S domain is disordered in the *B. stearothermophilus* crystal structure. This establishment of global stability by long-range, often phylogenetically volatile, structural elements probably explains why synthetic RNAs comprising only highly conserved core substructures are generally conformationally unstable.

The stabilization of global structure by helical struts reflects a general principle of RNA packing: unlike globular proteins, functional RNAs do not rely on the formation of a hydrophobic core to achieve a defined structure. Instead, in folded RNAs, double-stranded helical barrels are arranged by docking interactions that occur on the surface of the RNAs and involve a growing number of RNA structural motifs[70–72]. In the context of bacterial RNase P RNA, long-range docking interactions can be phylogenetically volatile (for example, helix P14), and different and unrelated structures can perform

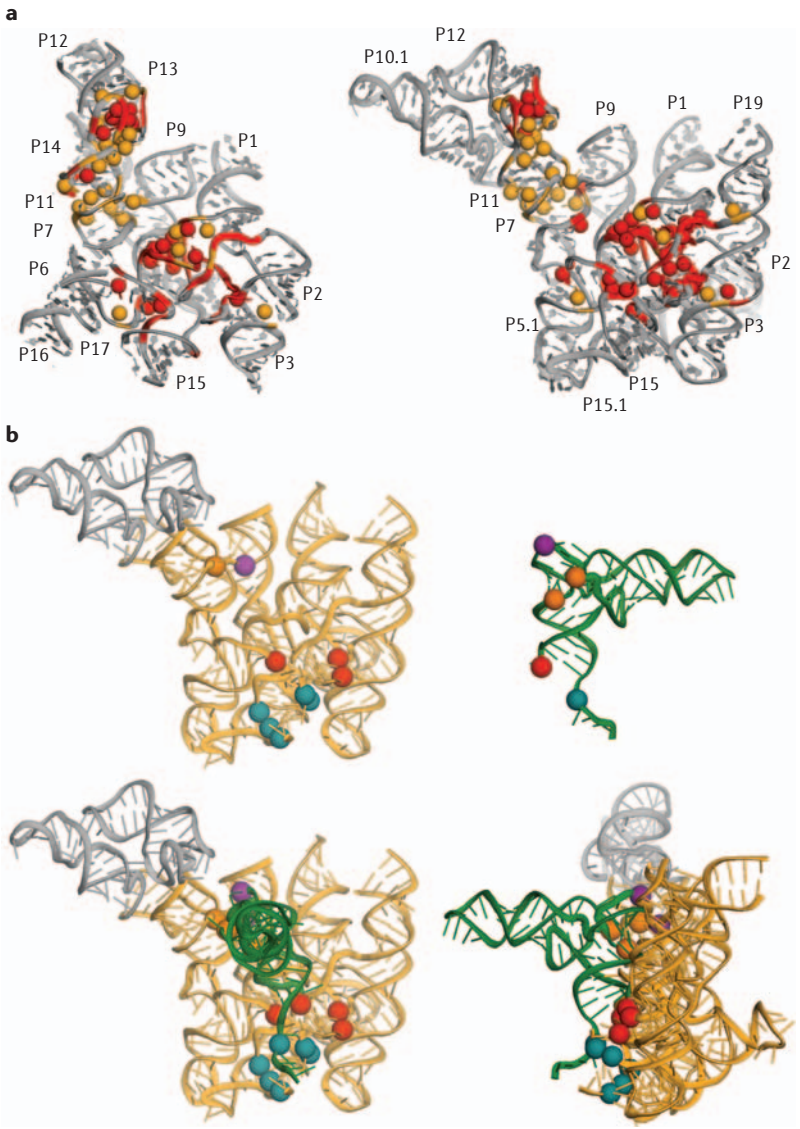

Figure 4 | **Conserved nucleotides in the bacterial RNase P RNA and reconstruction of the RNase P RNA complex. a** | Comparison of the distribution of the conserved nucleotides in the structures of A-type ribonuclease P (RNase P) RNA (left) and B-type RNase P RNA (right). Universally conserved nucleotides (represented by capital letters in the phylogenetic minimal structure in FIG. 2b) are shown in red. Highly conserved nucleotides (lower-case letters in the phylogenetic minimal structure in FIG. 2b) are shown in gold. Spheres indicate positions of the conserved nucleobases. **b** | Reconstruction of the RNase P RNA–tRNA complex by analysis of photo-affinity crosslinking data. The RNase P RNA is shown in grey and gold and transfer RNA (tRNA) is shown in green. In the top panel, the photoagent that is attached at different sites in the tRNA (shown as coloured spheres in the tRNA model on the right) forms crosslinks with different regions of the RNase P RNA (shown as spheres in the *B. stearothermophilus* RNase P RNA model on the left). The sites that crosslink with each other are represented by spheres of the same colour. The bottom row shows two different views of the reconstructed RNase P RNA–tRNA complex.

equivalent stabilizing tasks in the different structural types of the RNA. For instance, in one well-studied case, docking between P12 and P13 in the A-type RNase P RNA is replaced by a docking interaction of P10.1 to P12 in the B-type RNA[66]. Another example is the P16–P17–P6 structure in the A-type RNase P RNA, which does not occur in the B-type RNA. Instead, this structurally stabilizing strut is replaced in the B-type RNA by the structurally unrelated elements P5.1 and P15.1, which dock with each other by A-minor interactions and cross-strand stacking and occupy the same space in the overall structure as the A-type P16–P17–P6 structure[64].

Most of the structural motifs that form the long-range docking interactions in RNase P structures have been observed in different contexts in other RNA structures. These motifs include tetraloops and tetraloop receptors[73,74], ribose zippers[75], A-minor interactions[76], dinucleotide platforms[77,78] and others[63,64,66,67]. Two of the highly conserved structural features in RNase P RNAs have not been observed in any other RNA structure. One of these is formed by the highly conserved regions CRII and CRIII in the S domain, which form two intertwined T-loop-like structures[79]. Another is formed by the universally conserved helix P4 and five adjacent, highly conserved, interhelical joining regions, including phylogenetically absolutely conserved sequences in CRI, CRIV and CRV. The phylogenetic and biochemical data indicate that this complex structure contains the catalytic core of RNase P.

Even at the current resolution the crystal structures provide a new perspective on RNase P RNA. It is likely that the detail of the RNase P structure will be known only when the structure of the ternary complex, which includes the protein and pre-tRNA substrate, becomes available. Although not yet resolved crystallographically, the individual structures of these other elements are known and can be modelled onto the RNase P RNA, based on phylogenetic and biochemical criteria.

Modelling tRNA onto the ribozyme

The distribution of conserved nucleotides in the bacterial RNase P RNA structure provides a perspective on the important nucleobases and is shown in FIG. 4a. Two main areas of very high conservation are located in the S domain (CRII and CRIII) and the catalytic core (CRI, CRIV, CRV and a few other highly conserved nucleotides), connected by a region of less conserved structure. The distribution of conserved nucleotides seems to reflect the conservation of structure required to mould the substrate-binding patch in the RNase P RNA. This is supported by crosslinking studies (described below) and by the spatial distribution of chemical groups identified by nucleotide analogue interference mapping (NAIM) experiments as being important for substrate binding[80–85]: these tend to follow the distribution of the conserved nucleotides in FIG. 4a and again indicate the tRNA-binding pattern.

Intermolecular photo-affinity crosslinking data[54,55] provide specific distance measurements and so can be used in conjunction with the crystal structures to reconstruct, in general detail, a model of the complex that is formed between the RNA of RNase P and the tRNA product. In these crosslinking experiments an arylazide photoagent was attached to various sites throughout the tRNA structure. On ultraviolet (UV) irradiation of the complex between such derivatized tRNAs and RNase P RNA, the photoagent forms crosslinks with the nucleotides that are within 9 Å from the site of its

attachment in the overall structure. Crosslinked complexes of tRNA and RNase P RNA are then purified by gel electrophoresis and the sites of crosslinking in the RNase P RNA are identified by primer-extension analysis. The sites that are crosslinked from the variously positioned agents in tRNA to the RNase P RNA outline the tRNA-binding patch. Superimposition of the crystal structures of the tRNA and the RNase P RNA on the basis of the crosslinking constraints results in the model shown in FIG. 4b. This model is generally consistent with the distribution of the few known substrate-binding elements in the RNase P structure (see below). However, conformational rearrangements of the crystal structure might be indicated by some biochemically imposed constraints. For instance, a highly conserved nucleotide on the surface of the S domain is protected by tRNA from chemical modification[86,87], but this nucleotide is located ~11 Å from the nearest atom of the tRNA in the model of the complex.

The crystal structures, taken together with the data from photo-affinity crosslinking between the product phosphate and the ribozyme, provide the first glimpse of the structural organization of the chemically active site of RNase P. The crosslinked nucleotides[88] are localized in the highly conserved structure adjacent to helix P4 (FIG. 4b). Prior to the emergence of the crystal structures it was thought that the major groove of helix P4 might constitute the catalytically active site of RNase P because of its high conservation and the considerable biochemical and biophysical evidence indicating that P4 is involved in binding of catalytically important divalent metal ions[89–94]. The crosslinking data, however, convincingly place the product phosphate in the cleft formed by the interhelical joining regions that contain the highly conserved sequence elements CRIV and CRV. This assignment is further corroborated by analysis of the spatial distribution of the structural elements that are known to be involved in substrate recognition (see below).

Adding the protein to the complex

The structures of the protein components of diverse bacterial RNase P RNAs have been studied by X-ray crystallography[95,96] and NMR[97]. The protein components of both A-type and B-type RNase P are highly similar and, indeed, RNase P proteins from bacteria with A-type RNase P can functionally complement the B-type RNA *in vitro* as well as *in vivo*[7,98]. The proteins adopt a ribonucleoprotein-like fold of an α–β sandwich and have a highly conserved electrostatic surface matrix (FIG. 5b). This high degree of structural and functional conservation indicates that the bacterial RNase P protein binds to a region that is structurally conserved among all bacterial RNase P RNAs. One peculiar structural feature of the bacterial RNase P protein is an unusual left-handed β–α–β crossover that is also seen among related RNA-binding motifs of the ribosomal protein S5 superfamily[95]. This structural crossover contains a highly conserved 'RNR' sequence motif that contributes to formation of a highly positively charged surface on one side of the protein (FIG. 5b).

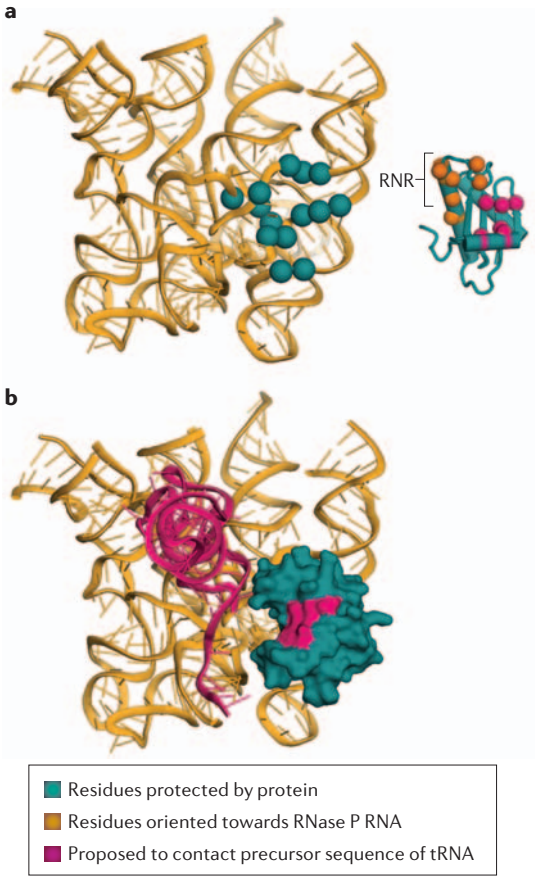

Figure 5 | **Modelling of the bacterial RNase P holoenzyme structure and its complex with tRNA.** **a** | Distribution of the biochemical data used for modelling the structures of ribonuclease P (RNase P) RNA and protein components. The model on the left shows the footprints left by diverse bacterial proteins on the RNase P RNA. Protein-dependent sites of protection from oxidation of phosphorothioate modifications in the RNA are shown as teal spheres. The schematic on the right shows the putative RNA-binding regions in the bacterial RNase P protein structure. Orange spheres indicate protein residues that are oriented towards RNase P RNA in the holoenzyme. Magenta spheres indicate residues that are proximal to the 5′ precursor of pre-tRNA in the holoenzyme–substrate complex. The highly conserved RNR motif is indicated by a bracket. **b** | Reconstructed model of the RNase P ternary complex. RNase P RNA is shown as a gold ribbon, transfer RNA (tRNA) is shown as a magenta ribbon. RNase P protein is shown in teal; the magenta patch indicates the residues that are proposed to contact the 5′ precursor of pre-tRNA in the holoenzyme–substrate complex.

Mutational[99] and biochemical data[100–102] implicate this positively charged face in binding to the RNase P RNA. Another characteristic structural feature of the bacterial RNase P proteins is a cleft formed by an N-terminal helix α-1 and the central β sheet. Mutational[99], photo-affinity crosslinking[103] and NMR studies[97] indicate that the 5′-leader sequence binds to this cleft on binding of the substrate pre-tRNA to the RNase P holoenzyme.

A-minor interaction
A common long-range interaction in structured RNA molecules achieved by docking of a bulged nucleotide (usually adenine) into a minor groove of a double-stranded helical structure. Four types of A-minor interactions are known; not all are specific for adenine. A-minor interactions are considered to be a subclass of ribose-zipper interactions.

Tetraloop
A four-base loop that caps a hairpin helix. Tetraloops often dock into other structural elements of RNA to provide long-range structural stability.

Ribose zipper
An element of RNA structure that is characterized by consecutive hydrogen-bonding interactions between ribose 2′-hydroxyls from different regions of an RNA chain or between RNA chains.

Dinucleotide platform
A structural feature in which folding of the RNA chain results in an in-plane, side-by-side positioning of consecutive bases.

Nucleotide analogue interference mapping
(NAIM). A technique that involves random, but sequence-specific, incorporation of chemical modifications into a pool of RNA molecules (usually achieved by *in vitro* transcription in the presence of nucleotide analogues) that is followed by a selection for a certain property (for example, folding, catalytic activity or ligand binding). Biochemical analysis of the distribution of such modifications reveals sites in RNA where the chemical modification interferes with the RNA property of interest.

S5 superfamily
A protein structural family that includes proteins and protein domains with a similar α–β-sandwich-like fold. The family is named after one of its members, a small subunit ribosomal protein S5.

Although considerable information has been available to infer which face of the protein interacts with the RNA in the complex[101,102], the site in the RNA to which the protein binds remained elusive until recently. A significant effort had been made over the years to identify the protein-binding site on the RNase P RNA by footprint analyses, in which RNA residues that are protected by the protein from chemical or enzymatic action are identified. The results obtained by different research groups[104–107] were inconsistent, presumably owing to factors such as nonspecific binding of excess RNase P protein, conformational heterogeneity in the RNA and aggregation of the holoenzyme. Such caveats were recently alleviated by chemical-footprinting experiments with RNAs and RNA–protein complexes following their resolution by native-gel electrophoresis[108]. In these assays, for the patch of RNA structure occupied by the protein, non-bridging phosphorothioate nucleotides were randomly incorporated into the RNase P RNA by *in vitro* transcription. These randomly modified RNAs were radioactively end-labelled, the native RNAs or holoenzymes were separated from incorrect forms by electrophoresis in native-polyacrylamide gels and were then subjected to oxidation with iodine in the gel to preserve the structure. Iodine breaks the RNA chain at the phosphorothioate bond unless it is somehow protected, and the sizes of the fragments reveal the break points. Analysis of A-type and B-type RNAs showed a common patch of protection that is distributed in the sequence but drawn together in the tertiary structure (FIG. 5a).

These biochemical data can be used to reconstruct the overall organization of the bacterial RNase P holoenzyme from the individual crystal structures of the RNA and protein, as shown in FIG. 5[108]. The model presumes that no significant conformational rearrangements occur on formation of the holoenzyme. The identified protein-binding site on RNase P RNA is located adjacent to, instead of precisely at, the proposed chemically active site. This position is in accordance with biochemical data that implicate the protein component in binding of the 5′-leader sequence[103]. The result is also consistent with the general belief that the bacterial RNase P protein has no direct role in catalysis.

Substrate recognition

A distinctive feature of the interaction of bacterial RNase P and its substrates is that there does not seem to be any primary recognition determinant, such as a particular sequence for substrate identification. Instead, recognition is achieved by contributions from a few enzyme–substrate interactions that are scattered on the binding faces and contribute cooperatively to substrate affinity and the correct selection of the site of hydrolysis.

RNase P binds the substrate along the coaxially stacked helical domain formed by the T-stem loop and the acceptor helix of the tRNA[109–111]. The anticodon and D-stem loops are not directly involved in binding and their absence from synthetic substrates has little influence on activity. Known recognition determinants include the T loop and the T stem and a few nucleotides that are located structurally proximal to the cleavage site, including the 3′-CCA of the tRNA and the 5′-leader sequence. Structure-based modelling of the complex of the enzyme with the product tRNA has indicated that the backbone of the acceptor stem might also contribute to substrate recognition. The atomic details of these interactions are not known, but biochemical studies provide some insights. For instance, conversion of a handful of 2′-OHs in the T loop, T stem and the 3′-CCA of pre-tRNA into 2′–3′-cyclophosphates interferes with its effective processing by RNase P RNA and indicates the importance of 2′-OH contacts[112]. Further analysis indicates that two highly conserved adenosines that bulge from the S domain of RNase P RNA (A130 in the base of helix P9 and A230 in the base of helix P11 in *B. subtilis*) might participate in docking with the T-stem loop[112,113]. Participation of the S domain of RNase P RNA in the interaction with the T-stem loop of the pre-tRNA is corroborated by photo-affinity crosslinking experiments[55], but the mechanism involved is not known.

The 3′-terminal CCA of pre-tRNA can be an important recognition determinant[114–116]. However, 3′-CCA is often not encoded by bacterial pre-tRNA genes and in these cases the CCA sequence is thought to be formed subsequent to the maturation of the 5′ end of pre-tRNA by an enzymatic pathway that involves RNase Z and terminal nucleotidyl transferase[117–119]. With pre-tRNAs that contain the 3′-CCA, this sequence is thought to pair with bases in the highly conserved loop L15 of the RNase P RNA[120–122]. The interaction of the 3′-CCA with L15 seems crucial for the correct selection of the site of processing[123], and is likely to be more complex than simple base pairing. For instance, nucleotide analogues that are incorporated at the position adjacent to the 3′-CCA of pre-tRNA interfere with binding of a Mg^{2+} ion that contributes to the overall Mg^{2+}-cooperativity of the RNase P reaction[122,124].

Another set of binding interactions that are important for processing-site selection involves the 5′-leader sequence. The N_{-1} nucleotide of the 5′-leader sequence interacts with an absolutely conserved adenosine in the J5–15 interhelical junction of RNase P RNA[125,126]. The N_{-2} of the 5′-leader sequence might also be important in binding[127–129], however, possible interaction partners in the RNase P are at present unknown. Longer 5′-precursor sequences seem to interact with the protein component of the RNase P holoenzyme[103], perhaps causing the 5′-precursor sequence to adopt an extended conformation in the complex with the holoenzyme[130].

The crystallographic[64] and photo-affinity crosslinking studies[131] indicate that another structural element in RNase P RNA, helix P4, must be important for correct binding of the substrate. Helix P4 is among the most highly conserved structures in the RNase P RNA molecule, and before crystallographic results, P4 was thought to be part of the chemically active site. Biochemical and physical data had implicated the major groove of helix P4 in loading divalent metal ions into the active site of the ribozyme[89–94]. However, the structural data summarized above locate helix P4 between the proposed

chemically active site and the T-loop-binding elements in the RNase P RNA, placing the metal-binding sites in the major groove of the helix P4 at least 15 Å away from the chemically active site. Consequently, the primary function of these metal-binding sites is probably to accommodate and correctly position the negatively charged backbone of the substrate-acceptor stem on substrate binding[131]. The RNA chains of both enzyme and substrate are highly negatively charged and their close proximity creates intense repulsion that must be screened by divalent cations for a proper fit to be achieved. This interaction between the substrate and helix P4 probably contributes significantly to substrate specificity and perhaps explains the high degree of conservation of that helix.

Conclusions

Crystallographic studies are painting an increasingly well-refined picture of the structural organization of RNase P RNA and its functional complexes. But the fact remains that we still do not have a real understanding of how RNase P RNA participates in the chemistry of the reaction. Perhaps, in the end, the conservation of the RNase P RNA structure simply serves to position the catalytically important divalent metal ions correctly, with no involvement of nucleobases in the chemistry of the process. RNase P RNA then would fulfil Yarus's 'Cheshire Cat' hypothesis, in which the organic component of RNA fades into the background, leaving only the mineral teeth[132].

Despite the progress with crystallographic studies of RNase P in recent years, we are far from understanding its structure. The true details of the interaction of RNA with the protein component and with the substrate are still unknown. The reconstructed structure shown in FIG. 5, although composed of the crystal structures of the individual components, is based on biochemical data and lacks the required level of precision. Future structural studies can be anticipated that will include the ternary complexes between the holoenzyme and substrate analogues.

1. Frank, D. N. & Pace, N. R. Ribonuclease P: unity and diversity in a tRNA processing ribozyme. *Annu. Rev. Biochem.* **67**, 153–180 (1998).
2. Walker, S. C. & Engelke, D. R. Ribonuclease P: the evolution of an ancient RNA enzyme. *Crit. Rev. Biochem. Mol. Biol.* **41**, 77–102 (2006).
3. Guerrier-Takada, C., Gardiner, K., Marsh, T., Pace, N. & Altman, S. The RNA moiety of ribonuclease P is the catalytic subunit of the enzyme. *Cell* **35**, 849–857 (1983).
Reports the discovery that the RNA of bacterial RNase P is catalytically proficient in the absence of the protein moiety of the enzyme.
4. Pannucci, J. A., Haas, E. S., Hall, T. A., Harris, J. K. & Brown, J. W. RNase P RNAs from some archaea are catalytically active. *Proc. Natl Acad. Sci. USA* **96**, 7803–7808 (1999).
5. Schedl, P. & Primakoff, P. Mutants of *Escherichia coli* thermosensitive for the synthesis of transfer RNA. *Proc. Natl Acad. Sci. USA* **70**, 2091–2095 (1973).
6. Apirion, D. Genetic mapping and some characterization of the *rnpA49* mutation of *Escherichia coli* that affects the RNA-processing enzyme ribonuclease P. *Genetics* **94**, 291–299 (1980).
7. Waugh, D. S. & Pace, N. R. Complementation of an RNase P RNA (*rnpB*) gene deletion in *Escherichia coli* by homologous genes from distantly related eubacteria. *J. Bacteriol.* **172**, 6316–6322 (1990).
8. Chamberlain, J. R., Lee, Y., Lane, W. S. & Engelke, D. R. Purification and characterization of the nuclear RNase P holoenzyme complex reveals extensive subunit overlap with RNase MRP. *Genes Dev.* **12**, 1678–1690 (1998).
The most thorough of the studies of the eukaryal RNase P.
9. Hartmann, E. & Hartmann, R. K. The enigma of ribonuclease P evolution. *Trends Genet.* **19**, 561–569 (2003).
10. Jarrous, N. Human ribonuclease P: subunits, function, and intranuclear localization. *RNA* **8**, 1–7 (2002).
11. Evans, D., Marquez, S. M. & Pace, N. R. RNase P: interface of the RNA and protein worlds. *Trends Biochem. Sci.* **31**, 333–341 (2006).
12. Kirsebom, L. A. RNase P RNA-mediated catalysis. *Biochem. Soc. Trans.* **30**, 1153–1158 (2002).
13. Harris, M. E. & Christian, E. L. Recent insights into the structure and function of the ribonucleoprotein enzyme ribonuclease P. *Curr. Opin. Struct. Biol.* **13**, 325–333 (2003).
14. Torres-Larios, A., Swinger, K. K., Pan, T. & Mondragon, A. Structure of ribonuclease P — a universal ribozyme. *Curr. Opin. Struct. Biol.* **16**, 327–335 (2006).
15. Peck-Miller, K. A. & Altman, S. Kinetics of the processing of the precursor to 4.5S RNA, a naturally occurring substrate for RNase P from *Escherichia coli*. *J. Mol. Biol.* **221**, 1–5 (1991).
16. Bothwell, A. L. M., Stark, B. C. & Altman, S. Ribonuclease P substrate specificity: cleavage of a bacteriophage ø80-induced RNA. *Proc. Natl Acad. Sci. USA* **73**, 1912–1916 (1976).
17. Guerrier-Takada, C., Van Belkum, A., Pleij, C. W. & Altman, S. Novel reactions of RNase P with a tRNA-like structure in turnip yellow mosaic virus RNA. *Cell* **53**, 267–272 (1988).
18. Komine, Y., Kitabatake, M., Yokogawa, T., Nishikawa, K. & Inokuchi, H. A tRNA-like structure is present in 10Sa RNA, a small stable RNA from *Escherichia coli*. *Proc. Natl Acad. Sci. USA* **91**, 9223–9227 (1994).
19. Alifano, P. *et al.* Ribonuclease E provides substrates for ribonuclease P-dependent processing of a polycistronic mRNA. *Genes Dev.* **8**, 3021–3031 (1994).
20. Hartmann, R. K., Heinrich, J., Schlegl, J. & Schuster, H. Precursor of C4 antisense RNA of bacteriophages P1 and P7 is a substrate for RNase P of *Escherichia coli*. *Proc. Natl Acad. Sci. USA* **92**, 5822–5826 (1995).
21. Altman, S., Wesolowski, D., Guerrier-Takada, C. & Li, Y. RNase P cleaves transient structures in some riboswitches. *Proc. Natl Acad. Sci. USA* (2005).
22. Altman, S. & Smith, J. D. Tyrosine tRNA precursor molecule polynucleotide sequence. *Nature New Biol.* **233**, 35–39 (1971).
Reports the discovery of the processing enzyme RNase P. The 'P' stands for 'processing'.
23. Smith, D. & Pace, N. R. Multiple magnesium ions in the ribonuclease P reaction mechanism. *Biochemistry* **32**, 5273–5281 (1993).
24. Beebe, J. A. & Fierke, C. A. A kinetic mechanism for cleavage of precursor $tRNA^{Asp}$ catalyzed by the RNA component of *Bacillus subtilis* ribonuclease P. *Biochemistry* **33**, 10294–10304 (1994).
25. Persson, T., Cuzic, S. & Hartmann, R. K. Catalysis by RNase P RNA: unique features and unprecedented active site plasticity. *J. Biol. Chem.* **278**, 43394–43401 (2003).
26. Cassano, A. G., Anderson, V. E. & Harris, M. E. Analysis of solvent nucleophile isotope effects: evidence for concerted mechanisms and nucleophilic activation by metal coordination in nonenzymatic and ribozyme-catalyzed phosphodiester hydrolysis. *Biochemistry* **43**, 10547–10559 (2004).
27. Smith, D., Burgin, A. B., Haas, E. S. & Pace, N. R. Influence of metal ions on the ribonuclease P reaction. Distinguishing substrate binding from catalysis. *J. Biol. Chem.* **267**, 2429–2436 (1992).
28. Brannvall, M. & Kirsebom, L. A. Metal ion cooperativity in ribozyme cleavage of RNA. *Proc. Natl Acad. Sci. USA* **98**, 12943–12947 (2001).
29. Cuzic, S. & Hartmann, R. K. Studies on *Escherichia coli* RNase P RNA with Zn^{2+} as the catalytic cofactor. *Nucleic Acids Res.* **33**, 2464–2474 (2005).
30. Kikovska, E., Mikkelsen, N. E. & Kirsebom, L. A. The naturally *trans*-acting ribozyme RNase P RNA has leadzyme properties. *Nucleic Acids Res.* **33**, 6920–6930 (2005).
31. Beebe, J. A., Kurz, J. C. & Fierke, C. A. Magnesium ions are required by *Bacillus subtilis* ribonuclease P RNA for both binding and cleaving precursor $tRNA^{Asp}$. *Biochemistry* **35**, 10493–10505 (1996).
32. Pan, T. Higher order folding and domain analysis of the ribozyme from *Bacillus subtilis* ribonuclease P. *Biochemistry* **34**, 902–909 (1995).
Shows that the RNase P RNA structure consists of independently folding domains.
33. Fang, X. W., Pan, T. & Sosnick, T. R. Mg^{2+}-dependent folding of a large ribozyme without kinetic traps. *Nature Struct. Biol.* **6**, 1091–1095 (1999).
34. Kent, O., Chaulk, S. G. & Macmillan, A. M. Kinetic analysis of the M1 RNA folding pathway. *J. Mol. Biol.* **304**, 699–705 (2000).
35. Warnecke, J. M., Furste, J. P., Hardt, W. D., Erdmann, V. A. & Hartmann, R. K. Ribonuclease P (RNase P) RNA is converted to a Cd^{2+}-ribozyme by a single R_p-phosphorothioate modification in the precursor tRNA at the RNase P cleavage site. *Proc. Natl Acad. Sci. USA* **93**, 8924–8928 (1996).
36. Warnecke, J. M., Held, R., Busch, S. & Hartmann, R. K. Role of metal ions in the hydrolysis reaction catalyzed by RNase P RNA from *Bacillus subtilis*. *J. Mol. Biol.* **290**, 433–445 (1999).
37. Steitz, T. A. & Steitz, J. A. A general two-metal-ion mechanism for catalytic RNA. *Proc. Natl Acad. Sci. USA* **90**, 6498–6502 (1993).
A general model for two-metal-promoted *trans*-esterification involving the phosphodiester bond.
38. Yang, W., Lee, J. Y. & Nowotny, M. Making and breaking nucleic acids: two-Mg^{2+}-ion catalysis and substrate specificity. *Mol. Cell* **22**, 5–13 (2006).
39. Stahley, M. R. & Strobel, S. A. Structural evidence for a two-metal-ion mechanism of group I intron splicing. *Science* **309**, 1587–1590 (2005).
40. Brautigam, C. A. & Steitz, T. A. Structural and functional insights provided by crystal structures of DNA polymerases and their substrate complexes. *Curr. Opin. Struct. Biol.* **8**, 54–63 (1998).
41. Jager, J. & Pata, J. D. Getting a grip: polymerases and their substrate complexes. *Curr. Opin. Struct. Biol.* **9**, 21–28 (1999).
42. Nowotny, M., Gaidamakov, S. A., Crouch, R. J. & Yang, W. Crystal structures of RNase H bound to an RNA/DNA hybrid: substrate specificity and metal-dependent catalysis. *Cell* **121**, 1005–1016 (2005).
43. Pingoud, A., Fuxreiter, M., Pingoud, V. & Wende, W. Type II restriction endonucleases: structure and mechanism. *Cell. Mol. Life Sci.* **62**, 685–707 (2005).
44. Stoddard, B. L. Homing endonuclease structure and function. *Q. Rev. Biophys.* **38**, 49–95 (2005).

45. Fox, G. W. & Woese, C. R. 5S RNA secondary structure. *Nature* **256**, 505–507 (1975).
46. Pace, N. R., Smith, D. K., Olsen, G. J. & James, B. D. Phylogenetic comparative analysis and the secondary structure of ribonuclease P RNA — a review. *Gene* **82**, 65–75 (1989).
47. Brown, J. W. *et al.* Comparative analysis of ribonuclease P RNA using gene sequences from natural microbial populations reveals tertiary structural elements. *Proc. Natl Acad. Sci. USA* **93**, 3001–3006 (1996).
First sequence-comparative RNA-structure analysis based on genes from complex natural microbial communities.
48. Pace, N. R. & Brown, J. W. Evolutionary perspective on the structure and function of ribonuclease P, a ribozyme. *J. Bacteriol.* **177**, 1919–1928 (1995).
49. Haas, E. S. & Brown, J. W. Evolutionary variation in bacterial RNase P RNAs. *Nucleic Acids Res.* **26**, 4093–4099 (1998).
50. Siegel, R. W., Banta, A. B., Haas, E. S., Brown, J. W. & Pace, N. R. *Mycoplasma fermentans* simplifies our view of the catalytic core of ribonuclease P RNA. *RNA* **2**, 452–462 (1996).
51. Harris, M. E. *et al.* Use of photoaffinity crosslinking and molecular modeling to analyze the global architecture of ribonuclease P RNA. *EMBO J.* **13**, 3953–3963 (1994).
52. Westhof, E. & Altman, S. Three-dimensional working model of M1 RNA, the catalytic RNA subunit of ribonuclease P from *Escherichia coli*. *Proc. Natl Acad. Sci. USA* **91**, 5133–5137 (1994).
53. Harris, M. E., Kazantsev, A. V., Chen, J. L. & Pace, N. R. Analysis of the tertiary structure of the ribonuclease P ribozyme–substrate complex by site-specific photoaffinity crosslinking. *RNA* **3**, 561–576 (1997).
54. Thomas, B. C., Kazantsev, A. V., Chen, J. L. & Pace, N. R. Photoaffinity cross-linking and RNA structure analysis. *Methods Enzymol.* **318**, 136–147 (2000).
Methodological review of the photo-affinity crosslinking agents and modelling strategies used to determine large-scale RNA structure.
55. Chen, J. L., Nolan, J. M., Harris, M. E. & Pace, N. R. Comparative photocross-linking analysis of the tertiary structures of *Escherichia coli* and *Bacillus subtilis* RNase P RNAs. *EMBO J.* **17**, 1515–1525 (1998).
56. Massire, C., Jaeger, L. & Westhof, E. Derivation of the three-dimensional architecture of bacterial ribonuclease P RNAs from comparative sequence analysis. *J. Mol. Biol.* **279**, 773–793 (1998).
57. Chen, J. L. & Pace, N. R. Identification of the universally conserved core of ribonuclease P RNA. *RNA* **3**, 557–560 (1997).
58. Harris, J. K., Haas, E. S., Williams, D., Frank, D. N. & Brown, J. W. New insight into RNase P RNA structure from comparative analysis of the archaeal RNA. *RNA* **7**, 220–232 (2001).
59. Marquez, S. M. *et al.* Structural implications of novel diversity in eucaryal RNase P RNA. *RNA* **11**, 739–751 (2005).
60. Pfeiffer, T. *et al.* Effects of phosphorothioate modifications on precursor tRNA processing by eukaryotic RNase P enzymes. *J. Mol. Biol.* **298**, 559–565 (2000).
61. Thomas, B. C., Chamberlain, J., Engelke, D. R. & Gegenheimer, P. Evidence for an RNA-based catalytic mechanism in eukaryotic nuclear ribonuclease P. *RNA* **6**, 554–562 (2000).
62. Thomas, B. C., Li, X. & Gegenheimer, P. Chloroplast ribonuclease P does not utilize the ribozyme-type pre-tRNA cleavage mechanism. *RNA* **6**, 545–553 (2000).
63. Torres-Larios, A., Swinger, K. K., Krasilnikov, A. S., Pan, T. & Mondragon, A. Crystal structure of the RNA component of bacterial ribonuclease P. *Nature* **437**, 584–587 (2005).
A 3.8-Å X-ray crystal structure of an A-type RNase P RNA, that of *Thermotoga maritima*.
64. Kazantsev, A. V. *et al.* Crystal structure of a bacterial ribonuclease P RNA. *Proc. Natl Acad. Sci. USA* **102**, 13992–13997 (2005).
A 3.3-Å X-ray crystal structure of a B-type RNase P RNA, that of *Bacillus stearothermophilus*.
65. Loria, A. & Pan, T. Domain structure of the ribozyme from eubacterial ribonuclease P. *RNA* **2**, 551–563 (1996).
66. Krasilnikov, A. S., Xiao, Y., Pan, T. & Mondragon, A. Basis for structural diversity in homologous RNAs. *Science* **306**, 104–107 (2004).
67. Krasilnikov, A. S., Yang, X., Pan, T. & Mondragon, A. Crystal structure of the specificity domain of ribonuclease P. *Nature* **421**, 760–764 (2003).
68. Fang, X. W. *et al.* The *Bacillus subtilis* RNase P holoenzyme contains two RNase P RNA and two RNase P protein subunits. *RNA* **7**, 233–241 (2001).
69. Buck, A. H., Dalby, A. B., Poole, A. W., Kazantsev, A. V. & Pace, N. R. Protein activation of a ribozyme: the role of bacterial RNase P protein. *EMBO J.* **24**, 3360–3368 (2005).
70. Moore, P. B. Structural motifs in RNA. *Annu. Rev. Biochem.* **68**, 287–300 (1999).
71. Leontis, N. B. & Westhof, E. Analysis of RNA motifs. *Curr. Opin. Struct. Biol.* **13**, 300–308 (2003).
72. Holbrook, S. R. RNA structure: the long and the short of it. *Curr. Opin. Struct. Biol.* **15**, 302–308 (2005).
73. Cate, J. H. *et al.* Crystal structure of a group I ribozyme domain: principles of RNA packing. *Science* **273**, 1678–1685 (1996).
74. Tinoco, I., Jr. RNA enzymes: putting together a large ribozyme. *Curr. Biol.* **6**, 1374–1376 (1996).
75. Tamura, M. & Holbrook, S. R. Sequence and structural conservation in RNA ribose zippers. *J. Mol. Biol.* **320**, 455–474 (2002).
76. Nissen, P., Ippolito, J. A., Ban, N., Moore, P. B. & Steitz, T. A. RNA tertiary interactions in the large ribosomal subunit: the A-minor motif. *Proc. Natl Acad. Sci. USA* **98**, 4899–4903 (2001).
77. Cate, J. H. *et al.* RNA tertiary structure mediation by adenosine platforms. *Science* **273**, 1696–1699 (1996).
78. Klosterman, P. S., Hendrix, D. K., Tamura, M., Holbrook, S. R. & Brenner, S. E. Three-dimensional motifs from the SCOR, structural classification of RNA database: extruded strands, base triples, tetraloops and U-turns. *Nucleic Acids Res.* **32**, 2342–2352 (2004).
79. Krasilnikov, A. S. & Mondragon, A. On the occurrence of the T-loop RNA folding motif in large RNA molecules. *RNA* **9**, 640–643 (2003).
80. Hardt, W. D., Warnecke, J. M., Erdmann, V. A. & Hartmann, R. K. R_p-phosphorothioate modifications in RNase P RNA that interfere with tRNA binding. *EMBO J.* **14**, 2935–2944 (1995).
81. Hardt, W. D., Erdmann, V. A. & Hartmann, R. K. R_p-deoxy-phosphorothioate modification interference experiments identify 2′-OH groups in RNase P RNA that are crucial to tRNA binding. *RNA* **2**, 1189–1198 (1996).
82. Heide, C., Pfeiffer, T., Nolan, J. M. & Hartmann, R. K. Guanosine 2-NH_2 groups of *Escherichia coli* RNase P RNA involved in intramolecular tertiary contacts and direct interactions with tRNA. *RNA* **5**, 102–116 (1999).
83. Siew, D., Zahler, N. H., Cassano, A. G., Strobel, S. A. & Harris, M. E. Identification of adenosine functional groups involved in substrate binding by the ribonuclease P ribozyme. *Biochemistry* **38**, 1873–1883 (1999).
84. Heide, C., Busch, S., Feltens, R. & Hartmann, R. K. Distinct modes of mature and precursor tRNA binding to *Escherichia coli* RNase P RNA revealed by NAIM analyses. *RNA* **7**, 553–564 (2001).
85. Heide, C., Feltens, R. & Hartmann, R. K. Purine N7 groups that are crucial to the interaction of *Escherichia coli* RNase P RNA with tRNA. *RNA* **7**, 958–968 (2001).
86. Lagrandeur, T. E., Huttenhofer, A., Noller, H. F. & Pace, N. R. Phylogenetic comparative chemical footprint analysis of the interaction between ribonuclease P RNA and tRNA. *EMBO J.* **13**, 3945–3952 (1994).
87. Odell, L., Huang, V., Jakacka, M. & Pan, T. Interaction of structural modules in substrate binding by the ribozyme from *Bacillus subtilis* RNase P. *Nucleic Acids Res.* **26**, 3717–3723 (1998).
88. Burgin, A. B. & Pace, N. R. Mapping the active site of ribonuclease P RNA using a substrate containing a photoaffinity agent. *EMBO J.* **9**, 4111–4118 (1990).
89. Harris, M. E. & Pace, N. R. Identification of phosphates involved in catalysis by the ribozyme RNase P RNA. *RNA* **1**, 210–218 (1995).
90. Frank, D. N. & Pace, N. R. *In vitro* selection for altered divalent metal specificity in the RNase P RNA. *Proc. Natl Acad. Sci. USA* **94**, 14355–14360 (1997).
91. Christian, E. L., Kaye, N. M. & Harris, M. E. Helix P4 is a divalent metal ion binding site in the conserved core of the ribonuclease P ribozyme. *RNA* **6**, 511–519 (2000).
92. Schmitz, M. & Tinoco, I., Jr. Solution structure and metal-ion binding of the P4 element from bacterial RNase P RNA. *RNA* **6**, 1212–1225 (2000).
93. Christian, E. L., Kaye, N. M. & Harris, M. E. Evidence for a polynuclear metal ion binding site in the catalytic domain of ribonuclease P RNA. *EMBO J.* **21**, 2253–2262 (2002).
94. Crary, S. M., Kurz, J. C. & Fierke, C. A. Specific phosphorothioate substitutions probe the active site of *Bacillus subtilis* ribonuclease P. *RNA* **8**, 933–947 (2002).
95. Stams, T., Niranjanakumari, S., Fierke, C. A. & Christianson, D. W. Ribonuclease P protein structure: evolutionary origins in the translational apparatus. *Science* **280**, 752–755 (1998).
96. Kazantsev, A. V. *et al.* High-resolution structure of RNase P protein from *Thermotoga maritima*. *Proc. Natl Acad. Sci. USA* **100**, 7497–7502 (2003).
97. Spitzfaden, C. *et al.* The structure of ribonuclease P protein from *Staphylococcus aureus* reveals a unique binding site for single-stranded RNA. *J. Mol. Biol.* **295**, 105–115 (2000).
98. Wegscheid, B., Condon, C. & Hartmann, R. K. Type A and B RNase P RNAs are interchangeable *in vivo* despite substantial biophysical differences. *EMBO Rep.* **7**, 411–417 (2006).
99. Gopalan, V., Baxevanis, A. D., Landsman, D. & Altman, S. Analysis of the functional role of conserved residues in the protein subunit of ribonuclease P from *Escherichia coli*. *J. Mol. Biol.* **267**, 818–829 (1997).
100. Gopalan, V. *et al.* Mapping RNA–protein interactions in ribonuclease P from *Escherichia coli* using electron paramagnetic resonance spectroscopy. *Biochemistry* **38**, 1705–1714 (1999).
101. Biswas, R., Ledman, D. W., Fox, R. O., Altman, S. & Gopalan, V. Mapping RNA–protein interactions in ribonuclease P from *Escherichia coli* using disulfide-linked EDTA–Fe. *J. Mol. Biol.* **296**, 19–31 (2000).
102. Tsai, H. Y., Masquida, B., Biswas, R., Westhof, E. & Gopalan, V. Molecular modeling of the three-dimensional structure of the bacterial RNase P holoenzyme. *J. Mol. Biol.* **325**, 661–675 (2003).
103. Niranjanakumari, S., Stams, T., Crary, S. M., Christianson, D. W. & Fierke, C. A. Protein component of the ribozyme ribonuclease P alters substrate recognition by directly contacting precursor tRNA. *Proc. Natl Acad. Sci. USA* **95**, 15212–15217 (1998).
104. Westhof, E., Wesolowski, D. & Altman, S. Mapping in three dimensions of regions in a catalytic RNA protected from attack by an Fe(II)–EDTA reagent. *J. Mol. Biol.* **258**, 600–613 (1996).
105. Loria, A., Niranjanakumari, S., Fierke, C. A. & Pan, T. Recognition of a pre-tRNA substrate by the *Bacillus subtilis* RNase P holoenzyme. *Biochemistry* **37**, 15466–15473 (1998).
106. Sharkady, S. M. & Nolan, J. M. Bacterial ribonuclease P holoenzyme crosslinking analysis reveals protein interaction sites on the RNA subunit. *Nucleic Acids Res.* **29**, 3848–3856 (2001).
107. Rox, C., Feltens, R., Pfeiffer, T. & Hartmann, R. K. Potential contact sites between the protein and RNA subunit in the *Bacillus subtilis* RNase P holoenzyme. *J. Mol. Biol.* **315**, 551–560 (2002).
108. Buck, A. H., Kazantsev, A. V., Dalby, A. B. & Pace, N. R. Structural perspective on the activation of RNase P RNA by protein. *Nature Struct. Mol. Biol.* **12**, 958–964 (2005).
Describes an in-gel footprinting technique for distinguishing native versus denatured RNase P complexes.
109. McClain, W. H., Guerrier-Takada, C. & Altman, S. Model substrates for an RNA enzyme. *Science* **238**, 527–530 (1987).
Reports the first use of 'designed' substrates for RNase P RNA.
110. Svard, S. G. & Kirsebom, L. A. Several regions of a tRNA precursor determine the *Escherichia coli* RNase P cleavage site. *J. Mol. Biol.* **227**, 1019–1031 (1992).
111. Yuan, Y. & Altman, S. Substrate recognition by human RNase P: identification of small, model substrates for the enzyme. *EMBO J.* **14**, 159–168 (1995).
112. Pan, T., Loria, A. & Zhong, K. Probing of tertiary interactions in RNA: 2′-hydroxyl–base contacts between the RNase P RNA and pre-tRNA. *Proc. Natl Acad. Sci. USA* **92**, 12510–12514 (1995).
113. Loria, A. & Pan, T. Recognition of the T stem-loop of a pre-tRNA substrate by the ribozyme from *Bacillus subtilis* ribonuclease P. *Biochemistry* **36**, 6317–6325 (1997).
114. Kirsebom, L. A. & Svard, S. G. Base pairing between *Escherichia coli* RNase P RNA and its substrate. *EMBO J.* **13**, 4870–4876 (1994).
115. Oh, B. K. & Pace, N. R. Interaction of the 3′-end of tRNA with ribonuclease P RNA. *Nucleic Acids Res.* **22**, 4087–4094 (1994).

116. Hardt, W. D., Schlegl, J., Erdmann, V. A. & Hartmann, R. K. Kinetics and thermodynamics of the RNase P RNA cleavage reaction: analysis of tRNA 3′-end variants. *J. Mol. Biol.* **247**, 161–172 (1995).
117. Pellegrini, O., Nezzar, J., Marchfelder, A., Putzer, H. & Condon, C. Endonucleolytic processing of CCA-less tRNA precursors by RNase Z in *Bacillus subtilis*. *EMBO J.* **22**, 4534–4543 (2003).
118. Nakanishi, K. & Nureki, O. Recent progress of structural biology of tRNA processing and modification. *Mol. Cells* **19**, 157–166 (2005).
119. Vogel, A., Schilling, O., Spath, B. & Marchfelder, A. The tRNase Z family of proteins: physiological functions, substrate specificity and structural properties. *Biol. Chem.* **386**, 1253–1264 (2005).
120. Svard, S. G., Kagardt, U. & Kirsebom, L. A. Phylogenetic comparative mutational analysis of the base-pairing between RNase P RNA and its substrate. *RNA* **2**, 463–472 (1996).
121. Busch, S., Kirsebom, L. A., Notbohm, H. & Hartmann, R. K. Differential role of the intermolecular base-pairs G292–C_{75} and G293–C_{74} in the reaction catalyzed by *Escherichia coli* RNase P RNA. *J. Mol. Biol.* **299**, 941–951 (2000).
122. Brannvall, M., Pettersson, B. M. & Kirsebom, L. A. Importance of the +73/294 interaction in *Escherichia coli* RNase P RNA substrate complexes for cleavage and metal ion coordination. *J. Mol. Biol.* **325**, 697–709 (2003).
123. Brannvall, M. & Kirsebom, L. A. Complexity in orchestration of chemical groups near different cleavage sites in RNase P RNA mediated cleavage. *J. Mol. Biol.* (2005).
124. Brannvall, M., Kikovska, E. & Kirsebom, L. A. Cross talk between the +73/294 interaction and the cleavage site in RNase P RNA mediated cleavage. *Nucleic Acids Res.* **32**, 5418–5429 (2004).
125. Zahler, N. H., Christian, E. L. & Harris, M. E. Recognition of the 5′ leader of pre-tRNA substrates by the active site of ribonuclease P. *RNA* **9**, 734–745 (2003).
126. Zahler, N. H., Sun, L., Christian, E. L. & Harris, M. E. The pre-tRNA nucleotide base and 2′-hydroxyl at N_{-1} contribute to fidelity in tRNA processing by RNase P. *J. Mol. Biol.* **345**, 969–985 (2005).
127. Brannvall, M., Mattsson, J. G., Svard, S. G. & Kirsebom, L. A. RNase P RNA structure and cleavage reflect the primary structure of tRNA genes. *J. Mol. Biol.* **283**, 771–783 (1998).
128. Loria, A. & Pan, T. Recognition of the 5′ leader and the acceptor stem of a pre-tRNA substrate by the ribozyme from *Bacillus subtilis* RNase P. *Biochemistry* **37**, 10126–10133 (1998).
129. Hansen, A. *et al.* Exploring the minimal substrate requirements for *trans*-cleavage by RNase P holoenzymes from *Escherichia coli* and *Bacillus subtilis*. *Mol. Microbiol.* **41**, 131–143 (2001).
130. Rueda, D., Hsieh, J., Day-Storms, J. J., Fierke, C. A. & Walter, N. G. The 5′ leader of precursor $tRNA^{Asp}$ bound to the *Bacillus subtilis* RNase P holoenzyme has an extended conformation. *Biochemistry* **44**, 16130–16139 (2005).
131. Christian, E. L., Smith, K. M., Perera, N. & Harris, M. E. The P4 metal binding site in RNase P RNA affects active site metal affinity through substrate positioning. *RNA* **12**, 1463–1467 (2006).
132. Yarus, M. How many catalytic RNAs? Ions and the Cheshire Cat conjecture. *FASEB* **7**, 31–39 (1993).

Acknowledgements
The authors' research is supported by a grant from the National Institutes of Health.

Competing interests statement
The authors declare no competing financial interests.

DATABASES
The following terms in this article are linked online to:
Entrez Genome Project: http://www.ncbi.nlm.nih.gov/entrez/query.fcgi?db=genomeprj
Bacillus stearothermophilus | *Bacillus subtilis* | *Thermotoga maritima* | *Thermus thermophilus*

FURTHER INFORMATION
The Pace laboratory homepage: http://Pacelab.colorado.edu
Access to this links box is available online.